2010 IEEE International Conference on Robotics and Automation
Anchorage Convention District
May 3-8, 2010, Anchorage, Alaska, USA

Statistical Mobility Prediction for Planetary Surface Exploration Rovers in Uncertain Terrain

Genya Ishigami, Gaurav Kewlani, and Karl Iagnemma

Abstract — **Planetary surface exploration rovers must accurately and efficiently predict their mobility on natural, rough terrain. Most approaches to mobility prediction assume precise a priori knowledge of terrain physical parameters, however in practical scenarios knowledge of terrain parameters contains significant uncertainty. In this paper, a statistical method for mobility prediction that incorporates terrain uncertainty is presented. The proposed method consists of two techniques: a wheeled vehicle model for calculating vehicle dynamic motion and wheel-terrain interaction forces, and a stochastic response surface method (SRSM) for modeling of uncertainty. The proposed method generates a predicted motion path of the rover with confidence ellipses indicating the probable rover position due to uncertainty in terrain physical parameters. Rover orientations and wheel slippage are also predicted. The computational efficiency of SRSM as compared to conventional Monte Carlo methods is shown via numerical simulations. Experimental results of rover travel over sloped terrain in two different uncertain terrains are presented that confirms the utility of the proposed mobility prediction method.**

I. INTRODUCTION

Mobile robotics has been performing a significant role in scientific lunar/planetary surface exploration missions [1]. In such missions, mobile robots are required to predict their mobility to avoid hazards such as immobilizing wheel slip on loose sand, or collision with obstacles. This "mobility prediction problem" is thus important to the successful exploration on challenging terrain. Of particular interest is mobility prediction on sloped terrain, since travel on slopes can cause extreme longitudinal and lateral slips.

There have been significant works dealing with mobility predictions and analyses in the military community [2][3]. These works have primarily focused on empirical analysis of large (i.e. several ton gross vehicle weight) vehicles. Other works have been performed to predict the mobility of small mobile robots while considering interaction mechanics of a slipping wheel on deformable terrain. Jain et al. has developed the ROAMS simulator, which can be used for deterministic mobility prediction and includes models of terrain/vehicle interactions [4]. A multibody system for deterministic simulation of rover tire-soil interaction has also been demonstrated [5]. A terramechanics-based dynamic model for exploration rovers that considers wheel slip and traction forces has been developed [6].

These works have employed well-known dynamic and terramechanics models to calculate vehicle motion and wheel forces. However, these models assume prior knowledge of wheel-terrain interaction physical parameters (i.e. soil cohesion, internal friction angle, and others). In practical situations, mobile robots often traverse environments composed of terrain with unknown properties. These parameters can be estimated by on-board robotic sensor systems [7]-[9], however these estimated parameters remain subject to uncertainty. Some recent work has attempted to predict rover mobility on slopes via a learning-based approach [10], however this work does not explicitly consider uncertainty in terrain physical parameters.

Based on these observations, it can be asserted that practical approaches to mobility prediction should explicitly consider uncertainty in terrain physical parameters. A conventional technique for estimating a probability density function of a system's output response from uncertain input distributions is the Monte Carlo method [11][12]. This approach generally requires a large number of analytical or numerical simulation trials to obtain a probability distribution of an output metric(s) associated with ranges of uncertain input parameters. Monte Carlo methods are typically computationally expensive with computational cost increasing as the simulation model complexity increases. Structured sampling techniques such as Latin hypercube sampling [13][14] can be used to improve computational efficiency, however these gains may be modest for complex problems.

This paper proposes a statistical method for efficient mobility prediction consisting of two techniques: a wheeled vehicle model for calculating vehicle dynamic motion and wheel-terrain interaction forces, and a stochastic response surface method (SRSM) for modeling of uncertainty. In the wheeled vehicle model [6], a terramechanics-based approach is used to calculate interaction forces of slipping wheels on deformable soil, and a dynamic model is employed to simulate vehicle motion. SRSM [15][16] is used as a functional approximation technique to obtain an equivalent system model with reduced complexity. Generally, the use of SRSM can reduce the number and complexity of model simulation trials to generate output metric statistics, as compared to Monte Carlo methods. In this paper, the computational efficiency of SRSM is confirmed through the comparison with those of Standard Monte Carlo method and Latin Hypercube Sampling Monte Carlo method.

Experimental studies of the proposed statistical mobility prediction method are conducted for a slope traversal scenario in two different terrains. Here, two key terrain parameters, cohesion and internal friction angle, are chosen as uncertain parameters. The proposed method provides a prediction of rover motion with confidence ellipses indicating probability ranges of the predicted position due to terrain

Manuscript received September 15, 2009. This work was supported by Army Research Office under contract number W912HZ-08-C-0060.

The authors are with the Department of Mechanical Engineering, Massachusetts Institute of Technology, Cambridge, MA 02139 USA (phone: 617-258-8428; e-mail: {ishigami, gkewlani, kdi}@mit.edu).

parameter uncertainty. Further, the method predicts the rover's probable orientation and wheel slippage.

This paper is organized as follows: Section II describes the outline of the proposed mobility prediction method. Section III explains SRSM and confidence ellipse calculation. The wheeled vehicle model is briefly introduced in Section IV. Section V describes the comparison of computational efficiency between Monte Carlo methods and SRSM, and also presents an experimental study using the proposed method.

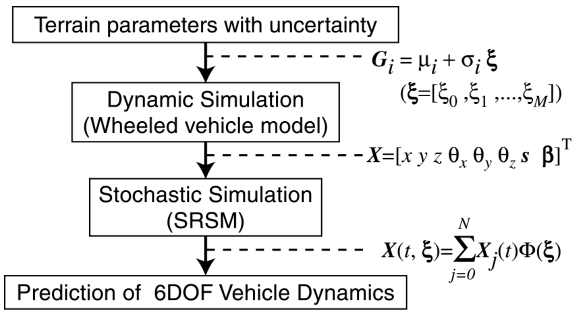

Fig.1. Flow chart of statistical mobility prediction method

II. OUTLINE OF STATISTICAL MOBILITY PREDICTION METHOD

Fig. 1 shows a flow chart of the statistical mobility prediction method proposed in this paper. This method is divided into three steps: First, uncertainty in terrain parameters $\boldsymbol{G}_i$ is represented as functions of standard random valuables (i.e. Gaussian variables):

$$\boldsymbol{G}_i = \mu_i + \sigma_i \boldsymbol{\xi} \tag{1}$$

where μ_i is the mean, σ_i is the standard deviation, and $\boldsymbol{\xi}$ is a set of standard normal random variables. Following the approach of [16], M sample points are calculated, where M is approximately twice the number of coefficients in SRSM reduced model (see (3) below).

In the second step, M dynamic simulations using the wheeled vehicle model are carried out to obtain several values for the variables of interest in a state space $\boldsymbol{X}$ corresponding to the uncertain inputs $\boldsymbol{G}_i$. The state space $\boldsymbol{X}$ consists of state variables of the vehicle, for example, vehicle position (x, y, z), vehicle orientation (θ_x, θ_y, θ_z), wheels' slip ratios $\boldsymbol{s}$, and wheels' slip angles $\boldsymbol{\beta}$:

$$\boldsymbol{X} = \begin{bmatrix} x & y & z & \theta_x & \theta_x & \theta_x & \boldsymbol{s} & \boldsymbol{\beta} \end{bmatrix} \tag{2}$$

In the third step, SRSM is employed to develop an equivalent reduced model of the state space, which can be expressed by:

$$\boldsymbol{X}(t,\boldsymbol{\xi}) = \sum_{j=0}^{N} \boldsymbol{X}_j(t)\boldsymbol{\Phi}_j(\boldsymbol{\xi}) \tag{3}$$

where $\boldsymbol{X}_j(t)$ is a set of unknown coefficient values that are calculated via a regression-based approach and $\boldsymbol{\Phi}_j(\boldsymbol{\xi})$ is a set of multidimensional Hermite polynomials with normal random variables. The number of unknown coefficients (N+1) is determined by both the degree q of polynomial expansion (see (5) below) and the number of the uncertain parameters. Once the coefficients are determined, the vehicle dynamic motion with terrain uncertainties can be predicted using the reduced model.

III. UNCERTAINTY ANALYSIS APPROACH

A. Stochastic Response Surface Method

SRSM provides a computationally efficient method for uncertainty propagation through the determination of a statistically equivalent reduced model [15][16]. In SRSM, inputs to a system model may be given as functions of independent identically distributed (iid) normal random variables, each having zero mean and unit variance (e.g. as defined in (1)). The same set of input random variables is then used for deriving the statistics of system model outputs.

An equivalent reduced model for output metrics is expressed as a series expansion in terms of standard random valuables as multidimensional Hermite polynomials with normal random variables:

$$y = a_0 + \sum_{i_1=1}^{n} a_{i_1}\Gamma_1(\xi_{i_1}) + \sum_{i_1=1}^{n}\sum_{i_2=1}^{i_1} a_{i_1}a_{i_2}\Gamma_2(\xi_{i_1},\xi_{i_2}) + \ldots \tag{4}$$

where y is an output metric, a_{i1}, a_{i2}...are unknown coefficients to be determined, and ξ_{i1}, ξ_{i2}...are iid normal random variables. The Hermite polynomial of degree q is given as:

$$\Gamma_q(\xi_{i_1},\xi_{i_2},....,\xi_{i_q}) = (-1)^q e^{\frac{1}{2}\boldsymbol{\xi}^T\boldsymbol{\xi}} \cdot \frac{\partial^q}{\partial\xi_{i_1},....,\partial\xi_{i_q}} \cdot e^{-\frac{1}{2}\boldsymbol{\xi}^T\boldsymbol{\xi}} \tag{5}$$

The accuracy of the model output increases as the order of the expansion q increases. For notational simplicity, the series in (4) can be rewritten as shown in (3):

$$y(t,\boldsymbol{\xi}) = \sum_{j=0}^{N} y_j(t)\boldsymbol{\Phi}_j(\boldsymbol{\xi}) \tag{6}$$

where the series is truncated to a finite number of terms and there exists a correspondence between $\Gamma_q(\xi_{i1}, \xi_{i2}, ..., \xi_{iq})$ and $\boldsymbol{\Phi}_j(\boldsymbol{\xi})$, and their corresponding coefficients. In this paper, the Hermite polynomial is used as the equivalent reduced model since input random variables are assumed to be Gaussian variables, however, different orthogonal polynomial basis functions can also be used for the probability distribution of other non-Gaussian variables [16].

The series expansion contains unknown coefficient values that can be determined from a limited number of system model simulations to generate an approximate reduced model. A set of sample points is selected and model outputs at these points are used for calculating the unknown coefficients. Once the statistically equivalent reduced model is formulated, it can be used to determine statistical properties related to mobility prediction, such as position and orientation of the vehicle subject to uncertainty.

B. Application of SRSM to Rover Mobility Prediction

In this paper, two key terrain parameters, cohesion c and internal friction angle ϕ, are chosen as uncertain variables. These parameters were chosen due to their influence on maximum terrain shear strength. These uncertain parameters are defined by the following normal distributions:

$$c = \mu_c + \sigma_c\xi_c, \qquad \phi = \mu_\phi + \sigma_\phi\xi_\phi \tag{7}$$

where μ_c and μ_ϕ are the means, σ_c and σ_ϕ are standard deviations, and ξ_c and ξ_ϕ are iid normal random valuables.

The output metrics considered in this paper include vehicle position, orientation, and wheel slippage, expressed as second order multidimensional Hermite polynomials:

$$\begin{aligned}\boldsymbol{X}(t,\boldsymbol{\xi}) &= \boldsymbol{X}_0(t) + \boldsymbol{X}_1(t)\xi_c + \boldsymbol{X}_2(t)\xi_\phi \\ &+ \boldsymbol{X}_3(t)(\xi_c^2 - 1) + \boldsymbol{X}_4(t)(\xi_\phi^2 - 1) + \boldsymbol{X}_5(t)\xi_c\xi_\phi\end{aligned} \quad (8)$$

where $\boldsymbol{X}_0(t)$, ..., $\boldsymbol{X}_5(t)$ are the unknown coefficient matrices.

Spectral stochastic analysis [17][18] is then performed using the expansion defined in (8) in order to obtain time series predictions of the motion path of the rover, and the vehicle orientations and wheel slippages.

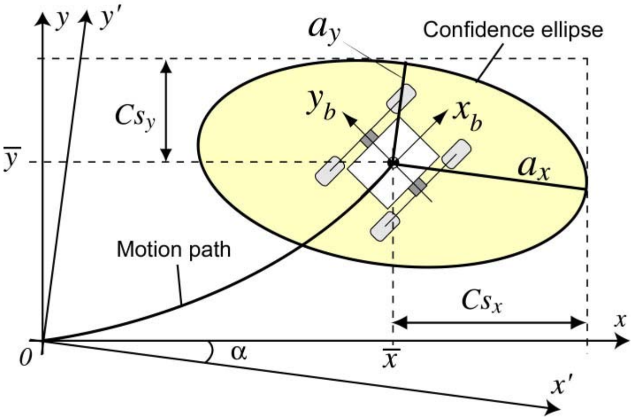

Fig.2. Confidence ellipse on the predicted motion path of the vehicle

C. Confidence Ellipse Calculation

Statistical techniques, such as Monte Carlo methods and SRSM, can provide predicted rover path coordinates (x, y) under uncertainty. Relevant output statistics such as the mean, variances, and covariance can also be calculated. Based on these statistics, the motion path (here taken as the mean path) can be augmented with ellipses defined by the variances and covariance (see Fig.2). The ellipses indicate confidence levels for the predicted position on the path. The confidence ellipse is drawn from the method presented in [19].

Given a sufficient sample size n from Monte Carlo methods or SRSM of motion path coordinates $\mathbf{x}_i = [x_i, y_i]^T$, a sample mean vector $\bar{\mathbf{x}}$ is given as:

$$\bar{\mathbf{x}} = [\bar{x}, \bar{y}]^T \quad (9)$$

where $\bar{x}$ and $\bar{y}$ are the means. The sample covariance matrix $\mathbf{S}$ is then determined as:

$$\mathbf{S} = \frac{1}{n-1}\sum_{i=1}^{n}(\mathbf{x}_i - \bar{\mathbf{x}})(\mathbf{x}_i - \bar{\mathbf{x}})^T = \begin{bmatrix} s_x^2 & rs_x s_y \\ rs_x s_y & s_y^2 \end{bmatrix} \quad (10)$$

where s_x and s_y are the sample standard deviations, s_{xy} is the sample covariance, and r is the sample correlation index.

The equation for a confidence ellipse is then formulated as:

$$(\mathbf{x} - \bar{\mathbf{x}})^T \mathbf{S}^{-1}(\mathbf{x} - \bar{\mathbf{x}}) = C^2 \quad (11)$$

where

$$C = \sqrt{-2\ln(1-P)} \quad (12)$$

P is the probability, which determines the confidence level of the predicted position.

Then, (11) can be rewritten by substituting (9) and (10):

$$\frac{1}{1-r^2}\left[\frac{(x-\bar{x})^2}{s_x^2} - \frac{2r(x-\bar{x})(y-\bar{y})}{s_x s_y} + \frac{(y-\bar{y})^2}{s_y^2}\right] = C^2 \quad (13)$$

As illustrated in Fig. 2, the principal semi-axes of the confidence ellipse for a given probability P are obtained from the following relationships:

$$a_x = Cs'_x, \quad a_y = Cs'_y \quad (14)$$

where a_x and a_y denote the major and minor semi-axes of the confidence ellipse. s'_x and s'_y are expressed by:

$$s'_{x,y} = \left\{\left[s_x^2 + s_y^2 \pm \sqrt{(s_x^2 - s_y^2)^2 + 4r^2 s_x^2 s_y^2}\right]\Big/2\right\}^{1/2} \quad (15)$$

The orientation of the confidence ellipse with regard to the x-y coordinate is defined by the inclination angle α:

$$\alpha = \frac{1}{2}\tan^{-1}\frac{2rs_x s_y}{s_x^2 - s_y^2} \quad (16)$$

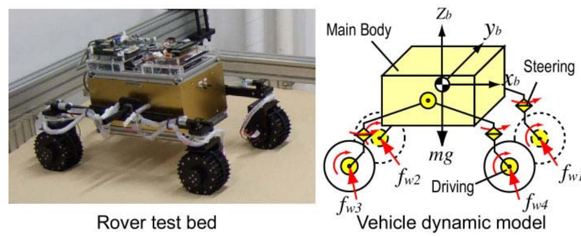

Fig.3. Vehicle dynamic model as an articulated multibody system

IV. WHEELED VEHICLE MODEL

Dynamic simulation of a wheeled rover requires two sub-models: a vehicle dynamic model of the rover to obtain several values for each state space variable, and a wheel-terrain contact model to calculate the interaction forces of a wheel on deformable soil at each dynamic simulation step. The wheeled vehicle model described in this section has been developed and validated in the authors' previous work [6].

A. Vehicle Dynamic Model

Here, a rover is modeled as an articulated multibody system. The vehicle addressed in this paper is assumed to be a 4-wheeled vehicle, as shown in Fig. 3.

The dynamic motion of a vehicle for given traveling and steering conditions are numerically obtained by successively solving the following motion equation:

$$\boldsymbol{H}\begin{bmatrix}\dot{\boldsymbol{v}}_0 \\ \dot{\boldsymbol{\omega}}_0 \\ \ddot{\boldsymbol{q}}\end{bmatrix} + \boldsymbol{C} + \boldsymbol{G} = \begin{bmatrix}\boldsymbol{F}_0 \\ \boldsymbol{N}_0 \\ \boldsymbol{\tau}\end{bmatrix} + \boldsymbol{J}^T\begin{bmatrix}\boldsymbol{F}_e \\ \boldsymbol{N}_e\end{bmatrix} \quad (17)$$

where $\boldsymbol{H}$ represents the inertia matrix of each body, $\boldsymbol{C}$ is the velocity depending term, $\boldsymbol{G}$ is the gravity term, $\boldsymbol{v}_0$ is the translational velocity of the vehicle, $\boldsymbol{\omega}_0$ is the angular velocity of the vehicle, $\boldsymbol{q}$ is the angle of each joint (such as wheel rotation and steering angle), $\boldsymbol{F}_0 = [0,0,0]^T$ is the forces at the centroid of the vehicle body, $\boldsymbol{N}_0 = [0,0,0]^T$ is the moments at the centroid of the vehicle body, $\boldsymbol{\tau}$ is the torques acting at each joint (wheel/steering torques), $\boldsymbol{J}$ is the Jacobian matrix, and $\boldsymbol{F}_e$ is the external forces acting at the centroid of each wheel. The wheel-terrain contact model, as described in (20)-(22) below, calculates each external force. $\boldsymbol{N}_e$ is the external moments acting at the centroid of each wheel.

B. Wheel-Terrain Contact Model

Wheel-terrain interaction mechanics has been well investigated in the field of terramechanics [20][21]. A model for a rigid wheel traveling on deformable soil is shown in Fig. 4. A wheel coordinate system is defined as a right-hand frame; in this system, the longitudinal direction is denoted by x_w, the lateral direction by y_w, and the vertical direction by z_w.

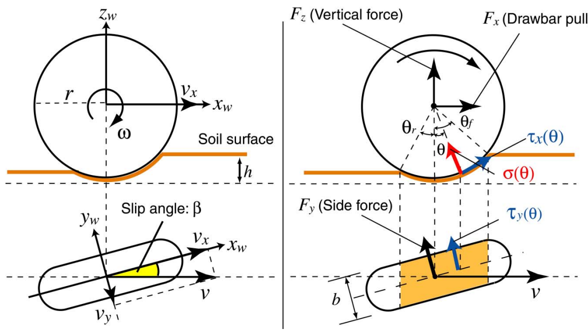

Fig.4. Wheel-terrain contact model for calculation of wheel forces

The slip ratio (i.e. slip in the longitudinal direction of wheel travel) is defined as a function of the longitudinal traveling velocity of the wheel v_x and the circumferential velocity of the wheel $r\omega$, where r is the wheel radius and ω represents the angular velocity of the wheel:

$$s = \begin{cases} (r\omega - v_x)/r\omega & (|r\omega| \geq |v_x| : \text{driving}) \\ (r\omega - v_x)/v_x & (|r\omega| < |v_x| : \text{braking}) \end{cases} \quad (18)$$

The slip ratio assumes a value in the range from –1 to 1.

The slip angle expresses the slip in the lateral direction of wheel and it is defined as a function of v_x and the lateral traveling velocity v_y, as follows:

$$\beta = \tan^{-1}(v_y / v_x) \quad (19)$$

Wheel-terrain contact forces, including the drawbar pull F_x, side force F_y, and vertical force F_z, can be calculated by the following equations [6][21]:

$$F_x = rb\int_{\theta_r}^{\theta_f} \{\tau_x(\theta)\cos\theta - \sigma(\theta)\sin\theta\} d\theta \quad (20)$$

$$F_y = \int_{\theta_r}^{\theta_f} \{rb\tau_y(\theta) + R_b r\cos\theta\} d\theta \quad (21)$$

$$F_z = rb\int_{\theta_r}^{\theta_f} \{\tau_x(\theta)\sin\theta + \sigma(\theta)\cos\theta\} d\theta \quad (22)$$

where b is the wheel width, $\sigma(\theta)$ is the normal stress beneath the wheel, $\tau_x(\theta)$ and $\tau_y(\theta)$ is the shear stresses in the longitudinal and lateral direction of the wheel. The contact patch of the wheel is determined by the entry angle θ_f and the exit angle θ_r. R_b is modeled as a reaction resistance generated by bulldozing phenomenon on a side wall of the wheel [6]. R_b is a function of the wheel sinkage h. Also, $\sigma(\theta)$, $\tau_x(\theta)$, and $\tau_y(\theta)$ are defined by the following equations [21]:

$$\sigma(\theta) = \begin{cases} (ck_c + \rho b k_\phi)\left(\frac{r}{b}\right)^n (\cos\theta - \cos\theta_f)^n \\ \quad (\theta_m \leq \theta < \theta_f) \\ (ck_c + \rho b k_\phi)\left(\frac{r}{b}\right)^n \left\{\cos\left[\theta_f - \frac{(\theta - \theta_r)(\theta_f - \theta_m)}{\theta_m - \theta_r}\right] - \cos\theta_f\right\}^n \\ \quad (\theta_r < \theta \leq \theta_m) \end{cases} \quad (23)$$

$$\left.\begin{aligned} \tau_x(\theta) &= [c + \sigma(\theta)\tan\phi][1 - e^{-j_x(\theta)/k_x}] \\ \tau_y(\theta) &= [c + \sigma(\theta)\tan\phi][1 - e^{-j_y(\theta)/k_y}] \end{aligned}\right\} \quad (24)$$

where k_c and k_ϕ represent the pressure sinkage moduli, ρ is the soil density, n is the sinkage exponent, θ_m is the maximum stress angle, c is the soil cohesion, ϕ is the soil internal friction, j_x and j_y are the soil shear deformations, and k_x and k_y are the soil deformation moduli.

From inspection of the above equations it is obvious that the terrain uncertainties addressed in this paper (cohesion c and internal friction angle ϕ) directly affect calculation of the normal and shear stresses, and result in uncertainty in wheel-terrain contact force calculation.

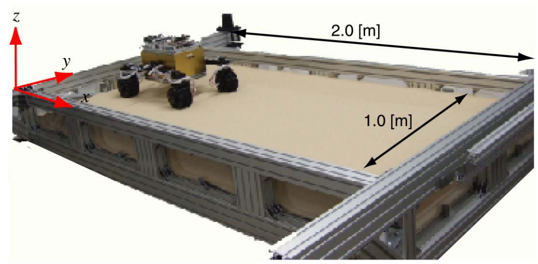

Fig.5. Mobility Prediction Scenario: Slope traversal with zero deg steering angles

TABLE I
STATISTICS OF UNCERTAIN TERRAIN PARAMETERS

Parameter (units)	Case A: Lunar simulant Mean	Case A: Lunar simulant Std. Dev.	Case B: Toyoura sand Mean	Case B: Toyoura sand Std. Dev.
c (kPa)	8.0	1.0	0.08	0.01
ϕ (deg)	37.2	4.65	38.0	2.38

TABLE II
TERRAIN PARAMETERS AND VALUES

Parameter	Value: Case A: Lunar simulant	Value: Case B: Toyoura sand	Unit
k_c	1.71	0.0	-
k_ϕ	4754.7	1203.5	-
ρ	1700.0	1490.5	kg/m^3
n	1.0	1.7	-
k_x	0.104	0.077	m
k_y	0.031	0.031	m

V. SIMULATION AND EXPERIMENTAL STUDIES OF MOBILITY PREDICTION PERFORMANCE

In the section, the computational efficiency of Standard Monte Carlo (SMC), Latin Hypercube Sampling Monte Carlo (LHSMC), and SRSM approaches are compared via simulation study. Then, an experimental study of the mobility prediction algorithm performance in two different terrains is described. The validity of the proposed technique is confirmed through the comparison between predicted and experimental motion paths of the rover.

A. Scenario Description

As shown in Fig.5, the mobility prediction scenario is one of a 4-wheeled rover traversing flat, sloped terrain with a side-slope angle of 10 deg, while maintaining 0 deg of steering angle at every wheel. The rover (see Fig.3) has dimensions of 0.44 m (length) x 0.30 m (width) x 0.30 m (height) and weighs 13.4 kg in total. Each wheel has a diameter of 0.11 m and a width of 0.06 m. The angular velocity of each wheel is controlled to maintain 0.3 rad/s.

The terrain surface of the slope is assumed to be evenly covered with two different types of soil: in Case A, the surface consists of the lunar regolith simulant [22], whereas in Case B, it is covered with cohesionless, Toyoura sand [23].

Uncertainties are represented in two critical terrain physical parameters, cohesion and internal friction angle. The mean and deviation of these parameters for the two soils of interest were determined by manual characterization, and are summarized in Table I. (Note that the mean and deviation can generally be estimated by engineering approximation, or predicted similarity to well-characterized soils.) Other parameters for calculation of the wheel-terrain interaction forces are summarized in Table II.

B. *Algorithm Flow of Mobility Prediction Method*

Rover mobility is predicted following the flow chart in Fig. 1. In this study, the probability distributions due to terrain uncertainty include the motion path during rover slope traversal, vehicle orientation, and wheel slippage.

The algorithm flow of the proposed mobility prediction method is summarized as follows:

1. Choose a sample value for the standard normal random variables ξ_c and ξ_ϕ, then calculate terrain parameters with uncertainty by (7).
2. Conduct slope traversal simulations over the set of uncertain terrain parameters $\boldsymbol{G}_i$:
   (a) Determine $\boldsymbol{\tau}$ such that the steering angle and wheel angular velocity are controlled to maintain their desired values;
   (b) Derive the external forces $\boldsymbol{F}_e$ acting at each wheel from the wheel-terrain contact model of (20)-(22);
   (c) Solve (17) to obtain the rover position, orientation, and velocity, then calculate the slip ratio and slip angle by (18) and (19).
3. Return to Step 1 until sufficient data sets of the state space $\boldsymbol{X}$ for calculation of the unknown coefficients are obtained. Taking the number of model simulation trials M to be approximately twice the number of unknown coefficients (N+1) has been shown to yield robust coefficient calculations [16][17].
4. Calculate the unknown coefficient matrices for the multidimensional Hermite polynomials using singular value decomposition and a regression-based approach.
5. Formulate a statistically equivalent reduced model as in (8) for the output uncertainty, then predict the rover position, orientations, and wheel slippages.
6. Calculate confidence ellipses based on (13) and draw a motion path with ellipses for visualization purposes.

C. *Simulation Results and Computational Efficiency*

Simulation results of the mobility prediction using SMC, LHSMC, and SRSM are briefly summarized as follows: The motion path obtained from SRSM is nearly identical to those obtained from SMC and LHSMC. The difference between the rover's final positions, as computed by SRSM and SMC, was 0.001 m in Case A, and that was 0.002 m in Case B. This result confirms that SRSM can provide a statistically equivalent representation of the complex system model considered in this analysis (i.e. the wheeled vehicle model).

Table III summarizes the computational time for mobility prediction between three approaches. These computations were performed on a 1.66 GHz laptop PC. The number of simulation runs of SMC was set as n=500, while that of LHSMC was n=100 since LHSMC secures more efficient sampling than SMC. The computational time of SRSM was approximately 71 times faster than that of SMC, and 14 times faster than LHSMC. This is due to the fact that SRSM avoids multiple runs of the nonlinear model, which results in reduced simulation time. Therefore, SRSM significantly improves the computational efficiency compared to the other methods.

For on-board usage of the proposed method, the wheeled vehicle model can be simplified as long as it provides equivalent performance to the accurate model so that the computational time will be reduced further. For example, the linear approximation of wheel stress model reported in [7] can reduce the complexity of wheel terrain contact model.

TABLE III
COMPUTATION TIME FOR MOBILITY PREDICTION ANALYSIS

Method	Case A: Lunar simulant	Case B: Toyoura sand
SMC (500 runs)	17526.1 sec	79994.1 sec
LHSMC (100 runs)	3507.2 sec	16232.5 sec
SRSM (2nd order)	245.8 sec	1125.9 sec

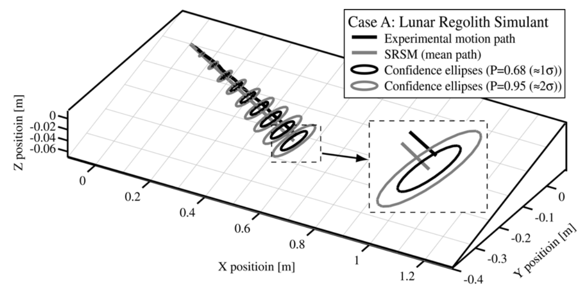

Fig.6. Mobility prediction of motion path with confidence ellipses, P = 68% (≈ 1σ) and P = 95% (≈ 2σ) , in Case A (Lunar regolith simulant

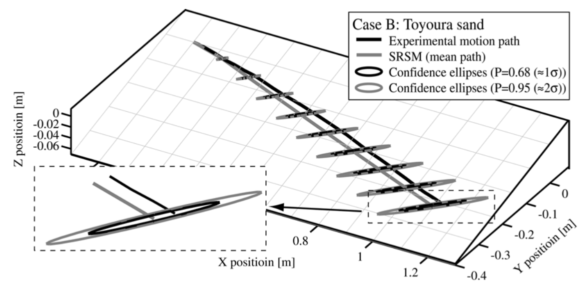

Fig.7. Mobility prediction of motion path with confidence ellipses, P = 68% (≈ 1σ) and P = 95% (≈ 2σ) , in Case B (Toyoura sand)

D. *Experimental Results and Discussions*

Statistical mobility predictions of the motion paths of the rover on two different types of soil are shown in Fig. 6 (Case A) and Fig. 7 (Case B) with experimental motion paths.

The solid black line depicts the experimental motion path, which was obtained via laboratory experimentation. The path was measured using a motion capture camera with positional accuracy of 0.01 m. Three experimental runs were performed for each soil. Here a typical result among them is presented

The predicted motion path of the rover obtained from SRSM is drawn as a gray line. Confidence ellipses were calculated with two different probabilities, P=68% (≈ 1σ), drawn as black ellipses, and P=95% (≈ 2σ), drawn as gray ellipses. These ellipses show the probable rover position considering uncertainty in terrain physical parameters. As expected, the 1σ confidence ellipses are smaller than the 2σ ellipses. The magnitude of the confidence level for mobility prediction can thus be "tuned" by the choice of probability.

In both cases, the experimental motion path falls within the predicted confidence ellipses, and in particular, the 1σ ellipses still contain the experimental results. This suggests that the proposed method can be used to reasonably predict rover motion. Viewed from another perspective, the results suggest that the actual (i.e. experimental) terrain parameters lie within the assumed ranges.

Mobility prediction results regarding the rover orientations (roll and yaw) and wheel slippage (at the front-left wheel of the rover) are summarized in Table IV. The predicted values include uncertainty bounds on the 2σ deviations. The deviations of the vehicle orientations are negligible in both cases, indicating that terrain uncertainty does not have significant influence on vehicle orientation in these cases.

The mean value of the wheel slip ratios are approximately 0.3~0.4, with small deviations in each case. However, the deviations of the slip angles are approximately 25% of their mean value. Since the deviation of the lateral wheel slip (measured by slip angle) is more significant than that of the longitudinal wheel slip (measured by slip ratio), deviation of the lateral vehicle position (depicted by the major axis of the confidence ellipses in Figs. 6-7) is larger than that of the longitudinal vehicle position (depicted by the ellipses' minor axes). Thus, as expected, for the case of slope traversal, uncertainty in terrain parameters largely contributes to the deviation in the lateral direction of the rover rather than in the longitudinal direction.

TABLE IV
MOBILITY PREDICTION RESULTS

Parameter	Case A: Lunar simulant		Case B: Toyoura sand	
(units)	Mean	2σ Dev.	Mean	2σ Dev.
Roll (deg)	10.1	0.00	13.3	0.01
Yaw (deg)	-0.17	0.17	9.58	0.09
Slip ratio (-)	0.43	0.03	0.29	0.08
Slip angle (deg)	-18.8	3.93	-14.5	4.20

VI. CONCLUSION

In this paper, a statistical mobility prediction for planetary surface exploration rovers has been described. This method explicitly considers uncertainty of the terrain physical parameters via SRSM, and employs models of both vehicle dynamics and wheel-terrain interaction mechanics.

The simulation results of mobility prediction using three different techniques, SMC, LHSMC, and SRSM, confirms that SRSM significantly improves the computational efficiency compared to those conventional methods.

The usefulness and validity of the proposed method has been confirmed through experimental studies of the slope traversal scenario in two different terrains. The results show that the predicted motion path with confidence ellipses can be used as a probabilistic reachability metric of the rover position. Also, for the slope traversal case, terrain parameter uncertainty has a larger influence on the lateral motion of the rover than on longitudinal motion.

Future directions of this study will apply the proposed technique to the path planning problem. There, confidence ellipses will be used to define collision-free areas, which will provide useful criteria for generating safe trajectories.

REFERENCES

[1] Mars Exploration Rover Mission [Online]. Available: http://marsrovers.jpl.nasa.gov/home/index.html.

[2] M. Jurkat, C. Nuttall, and P. Haley, *The AMC '74 Mobility Model,* Technical Report 11921, US Army Tank Automotive Command, Warren, MI, 1975.

[3] R. B. Ahlvin and P. W. Haley, *NATO Reference Mobility Model Edition II, NRMM User's Guide,* Technical Report GL-92-19, U.S. Army WES, Vicksburg, MS, 1992.

[4] A. Jain, J. Guineau, C. Lim, W. Lincoln, M. Pomerantz, G. Sohl, and R. Steele, "ROAMS: Planetary Surface Rover Simulation Environment," in *Proc. of 7th International Symposium on Artificial Intelligence, Robotics and Automation in Space, i-SAIRAS*, Nara, Japan, 2003.

[5] A. Gibbesch and B. Schäfer, "Multibody system modelling and simulation of planetary rover mobility on soft terrain," in *Proc. of 8th International Symposium on Artificial Intelligence, Robotics and Automation in Space, i-SAIRAS*, Munich, Germany, 2005.

[6] G. Ishigami, A. Miwa, K. Nagatani, and K. Yoshida, "Terramechanics-Based Model for Steering Maneuver of Planetary Exploration Rovers on Loose Soil," *Journal of Field Robotics*, vol. 24, no. 3, pp. 233–250, 2007.

[7] K. Iagnemma, S. Kang, H. Shibly, and S. Dubowsky, "Online terrain parameter estimation for wheeled mobile robots with application to planetary rovers," *IEEE Trans. on Robotics*, vol. 20, no. 5, pp.921–927, 2004

[8] J. Matijevic *et al.*, Characterization of Martian surface deposits by the Mars pathfinder rover, Sojourner," *Science*, vol. 278, no. 5, pp.1765–1768, 1997.

[9] S. Hutangkabodee, Y. Zweiri, L. Seneviratne, and K. Althoefer, "Soil parameter identification for wheel-terrain interaction dynamics and traversability prediction," *International Journal of Automation and Computing*, vol. 3, no. 3, pp.244–251, 2006.

[10] D. Helmick, A. Angelova, L. Matthies, C. Brooks, I. Halatci, S. Dubowsky, and K. Iagnemma, "Experimental Results from a Terrain Adaptive Navigation System for Planetary Rovers," in *Proc. of 9th International Symposium on Artificial Intelligence, Robotics and Automation in Space, i-SAIRAS*, Hollywood, CA, 2008.

[11] R. Rubinstein, *Simulation and the Monte Carlo Method*, John Wiley & Sons, Inc., 1981.

[12] M. Kalos and P. Whitlock, *Monte Carlo Methods, Vol. 1: Basics*, Wiley-Interscience, 1986.

[13] M. D. McKay, "Latin hypercube sampling as a tool in uncertainty analysis of computer models," in *Proc. of the 24th Conf. on Winter simulation*, pp.557-564, 1992.

[14] J. C. Helton and F. J. Davis, "Latin hypercube sampling and the propagation of uncertainty in analyses of complex systems," *Reliability Engineering and System Safety,* vol. 81 (1), 23-69, 2003

[15] S. Isukapalli, S. Balakrishnan, and P. Georgopoulos, "Computationally efficient uncertainty propagation and reduction using the stochastic response surface method," in *Proc. of the IEEE Conf. on Decision and Control*, Atlantis, Bahamas, 2004, pp. 2237–2243.

[16] S. Isukapalli, *Uncertainty analysis of transport-transformation models*, Ph.D. Thesis, Rutgers University, 1999.

[17] S. Huang, S. Mahadevan, and R. Rebba, "Collocation-based stochastic finite element analysis for random field problems," *Probabilistic Engineering Mechanics*, vol. 22, pp. 194-205, 2007.

[18] L. Li and C. Sandu, "On the impact of cargo weight, vehicle parameters, and terrain characteristics on the prediction of traction for off-road vehicles," *Journal of Terramechanics,* vol. 44, issue 3, pp.221-238, 2007.

[19] L. R. Paradowski, "Uncertainty Ellipses and Their Application to Interval Estimation of Emitter Position," *IEEE Trans. on Aerospace and Electronic Systems*, vol. 33, no. 1, pp.126-133, 1997.

[20] M. G. Bekker, *Introduction to Terrain-Vehicle Systems*, The University of Michigan Press, 1969.

[21] J. Y. Wong, *Theory of Ground Vehicles* (*3rd Edition*), John Wiley & Sons, 2001.

[22] H. Nakashima, Y. Shioji, K. Tateyama, S. Aoki, H. Kanamori, and T. Yokoyama, "Specific Cutting Resistance of Lunar Regolith. Simulant under Low Gravity Conditions," *Journal of Space Engineering*, vol. 1, no. 1, pp. 58-68, 2008.

[23] Toyoura Keiseiki Kogyo Co., Ltd. [Online]. Available: http://www.toyourakeiseki.com/product-e.htm.